Rates of Pyrolysis of Colorado Oil Shale

ZHENGLU PAN, H. Y. FENG
and J. M. SMITH
University of California
Davis, CA 95616

Both intrinsic kinetics and rates of decomposition in larger particles were determined for a Colorado shale by weight-loss measurements in TGA-type equipment. The data for small granular particles indicated first-order intrinsic kinetics up to a fractional weight change that depended on the temperature level. In the experiments with larger particles, gas, particle-surface, and particle-center temperatures measured in separate runs showed that both gas-to-particle and intraparticle temperature differences were significant.

A heat transfer model was evaluated by using the intrinsic kinetics data, measured heat transfer coefficients, and shale properties from the literature, to predict weight loss and particle-center temperatures for the larger particles. Comparison with observed results showed good agreement in general, although there was some deviation in weight-loss results at low temperatures.

The combined set of intrinsic kinetics data and rates for larger particles should be useful for further studies of pyrolysis models.

SCOPE

Our main objective was to provide a reasonably complete and consistent set of experimental data needed to analyze the rates of pyrolysis of Colorado oil shale. Thus, for the same shale, intrinsic kinetics were obtained from TGA experiments on small particles (48–60 mesh, average size 0.27×10^{-3} m) and weight vs. time data were obtained for cylindrical particles (2.54×10^{-2} m diam., 2.0×10^{-2} m length) where transport processes affected pyrolysis rates. Also gas, surface, and particle-center temperatures were measured for the cylindrical shale particles. In addition, gas-to-particle heat transfer coefficients were determined from dynamic temperature data on stainless steel cylinders of the same size and placed in the same apparatus.

While there have been several studies of kinetics using small particles, and weight and product distribution for larger particles, to our knowledge no data have been reported on both intrinsic kinetics and rates for larger particles (where transport processes influence the results) for the same shale. Hubbard and Robinson (1950) and Finucane et al. (1977) have measured intrinsic kinetics but have not presented data for large particles showing the effect of transport processes. These authors explained their data in terms of two successive first-order reactions. Allred (1966) proposed that decomposition reactions occurred in three stages, each with a different rate constant. On the other hand, Shih and Sohn (1980), Granoff and Nuttall (1977), and Nuttall et al. (1983), among others, have obtained pyrolysis rate data which included transport effects, but have not measured intrinsic kinetics. Decomposition rates have been studied by two methods: measuring sample weight vs. time and measuring product composition (usually gas, oil, and coke) as a function of time. For example, Johnson et al. (1975) described the production of products in terms of a set of ten parallel and series reactions. Intrinsic rate constants were given for each reaction, but no information was provided on transport effects.

To accomplish our objective, intrinsic rates were measured with the 48–60 mesh particles in a conventional thermogravimetric analysis (TGA) unit operated at constant temperature in the range 673–718 K. Then runs were made with the cylindrical particles; the sample weight was measured while the temperature was increased with time and then held constant at a plateau value. These experiments were carried out in a second, larger TGA apparatus and their purpose was to establish the combined effects of intrinsic kinetics and transport processes. In the work with cylinders, the surrounding gas, particle-surface, and particle-center temperatures were determined in separate experiments with the same size shale particles.

A secondary objective was to evaluate, by comparison with the experimental data, a two-dimensional heat transfer model for predicting both temperatures and weight vs. time. The experimental intrinsic kinetics and heat transfer coefficient data provided a severe test of modeling since no adjustable parameters were employed.

It should be emphasized that our objectives did not include attempts to interpret the intrinsic kinetics data in terms of a reaction sequence that would explain the production of various decomposition products. Rather, we used a simple, first-order rate equation which satisfactorily correlated the small-particle weight vs. time data up to kerogen decompositions of about 90%. However, both the small and large particle data should be useful to other investigators in evaluating more complex kinetics and modeling procedures.

CONCLUSIONS AND SIGNIFICANCE

We determined intrinsic kinetics for two Colorado shales from different locations from weight vs. time data obtained at temperatures from 673 to 718 K. The activation energies for the two shales were nearly the same. Since carbon (coke) is a product of pyrolysis, deposition of coke will affect the weight and the kinetics. Accordingly, first-order kinetics was followed over only part of the pyrolysis process. The fractional weight loss at which deviations from first-order behavior became significant depended upon the source of the shale and on the temperature of pyrolysis. For the leaner Anvil Points shale particles, first-order behavior was observed only down to a fractional weight loss of about 50% at 673 K, but this increased to 90% at 718 K. For the Clear Creek shale the figures were 90% at 673 K and 95% at 718 K.

An important conclusion from the temperature data for the cylindrical particles was that both gas-to-particle and intraparticle heat transfer affect pyrolysis rates. The maximum difference between particle-center and gas temperatures was about 60°C. Significant temperature differences occurred during most of the temperature-rising period and for much of the subsequent constant-temperature (gas temperature) period. It was during this time that most of the kerogen was pyrolyzed. Surface temperatures were difficult to reproduce, but the data indicated that the gas-to-particle temperature difference was somewhat larger than the difference between surface and center of the particle.

In the apparatus used for the large particles, the particles were located in a chamber in which the surrounding nitrogen was in swirling flow. In this environment the heat transfer coefficient from gas to particle increased only slightly with gas throughput and had an average value of about 36 $J/m^2 \cdot K \cdot s$.

The experimental intrinsic kinetics and heat transfer coefficient data, along with shale property data from the literature, were used with a two-dimensional heat transfer model to predict the temperature and sample weights for the large particles. Predicted particle-center temperatures were in good agreement with the measured values at all temperature levels. The predicted weight-loss results agreed with the experimental values at the highest plateau temperatures (711 K) but showed some deviations at lower temperatures. Part of the deviation is because first-order intrinsic kinetics was used in the model, and such kinetics did not fit the data at large fractional weight losses. A long time is required at low temperatures to pyrolyze all of the kerogen in the shale. If more coke is formed due to this long run time, this could also explain part of the deviation. Assumptions in the model and the need to use literature values for some shale properties introduced uncertainties in the predicted results. However, sensitivity calculations suggest that uncertainties in the properties would not explain the deviations of the predicted fractional weight losses at the lower plateau temperatures.

The major results of our research are the several kinds of experimental data for the same shale. These pyrolysis and heat transfer results should be useful in elucidating further the decomposition rates of kerogen.

INTRODUCTION

Visual examination of Colorado shale shows that the particles have a definite structure with more or less horizontal (with respect to the earth's surface) layers of dark material and lighter-colored rock. The dark material, kerogen, is a complex substance consisting of large molecules of carbon and hydrogen with nitrogen, sulfur, and oxygen atoms. The average molecular weight is of the order of 3,000 and an approximate empirical formula could be written $C_{200}H_{300}SN_5O_{11}$. When shale particles are heated to about 623 K, kerogen starts to decompose and partially vaporize, leading to final products which at room temperature consist of gas, oil, and residual carbon. For the design of equipment for obtaining oil from shale it is necessary to know the rate of decomposition. Except for small particles, such rates are expected to be influenced by transport processes as well as by intrinsic kinetics.

Experimental measurements with small particles have been approximately correlated by assuming first-order kinetics, as seen from the investigations of Shih and Sohn (1980), Hubbard and Robinson (1950), and Johnson et al. (1975). Overall kinetics can be obtained by measuring the change in weight of shale sample with time, as in thermogravimetric analysis (TGA) apparatus. Alternatively, rates of production of gas, oil, and carbon (coke) can be achieved by analyzing the products of retorting. The comprehensive study by Johnson et al. (1975) employed a scheme of ten parallel and successive reactions leading to products described as gas, oil, heavy oil, semicoke, and coke. First-order rate constants and activation energies were determined using this scheme and laboratory data.

Several studies—e.g., Granoff and Nuttall (1977); Shih and Sohn (1980); and Johnson et al. (1975)—have demonstrated that transport effects can affect global decomposition rates for large particles. Galan and Smith (1983) found such effects to become significant for granular particles larger than about 0.4×10^{-3} m. Johnson et al. (1975) considered both intraparticle heat and mass transfer and developed a model which accounted for intraparticle concentration and temperature gradients in an isotropic spherical particle (cylindrical geometry was also considered). Few details of the experiments are given, but product yields predicted from the model and intrinsic kinetics compared well with experimental yields for spherical particles as large as 0.10 m (4 in.).

Shih and Sohn (1980) employed available intrinsic kinetics data with a model that accounted for gas-to-particle and intraparticle heat transfer to produce overall rates of kerogen decomposition. Their model also was developed for an isotropic spherical particle. Mass transfer resistances were neglected. The computed results showed that the significance of intraparticle temperature gradients depended upon the heating rate (TGA experiments) and the gas velocity around the shale particles, as well as on particle size.

Granoff and Nuttall (1977) measured weight and temperature vs. time in a TGA apparatus for pyrolysis of shale particles in the shape of cylinders with length and diameter equal to 0.0127 m, and spheres of 0.0127 m diameter. Two models were tested with these data. The first was a shrinking-core, spherical particle model which took into account the layer structure of the kerogen in the particles and also accounted for gas-to-particle and intraparticle heat transfer. The second model assumed an isotropic particle and neglected intraparticle temperature gradients (uniform temperature model). Shih and Sohn (1980) applied their model for the spherical particles and operating conditions employed by Granoff and Nuttall. The predicted weight and temperature vs. time curves gave better agreement than the uniform temperature model. This comparison suggests that intraparticle temperature gradients significantly affected the decomposition rate for 0.0127 m particles. Literature information was used for intrinsic kinetics in all the predictions.

The purpose of the research reported here was to make a careful experimental and model study of the effects of heat transfer on rates of shale pyrolysis. To accomplish this objective, intrinsic kinetics was determined with small particles of the same shale as used to measure pyrolysis rates with large particles. Intrinsic kinetics was measured with small samples in a conventional TGA instrument, while pyrolysis of large particles was studied in a custom-made large TGA-type apparatus. To provide a more careful test of the predictive model, heat transfer coefficients from gas to particle were measured separately in the same large TGA-type apparatus. In retorting the large particles, weight and gas and particle temperatures were measured as a function of time. The mass transfer resistances from particle to gas and within the particle were assumed to be negligible in our model. Evidence for this assumption is discussed later.

EXPERIMENTAL

Two different samples of Colorado shale were studied. One was from the Anvil Points Mine, with a Fischer assay of 113×10^{-6} m^3 oil/kg shale (27 gal oil/ton of shale) and the second was a richer sample [Fischer assay $>125 \times 10^{-6}$ m^3 oil/kg (>30 gal/ton)] from the Clear Creek area, R7 zone. Additional properties are given in Table 1. Intrinsic kinetics data were

TABLE 1. PROPERTIES OF SHALE SAMPLES

Property	Anvil Points Mine*	Clear Creek R7 Zone**
Fisher assay, m^3/kg(gal/ton)	113×10^{-6}(27)	125×10^{-6}(30)
Analysis, wt, %		
Carbon (total)	21.70	
Hydrogen	2.38	
Nitrogen	0.66	
Sulfur	0.66	
Moisture	0.50	
Ash†	62.00	
Carbonate (CO_3)	23.30	
Oil, wt. %		11.40
Water, wt. %		2.10
Gas plus loss, wt. %		3.10

* From Occidental Research Corp.
** From Chevron Research Corp.
† Wt. of residue after heating in air to 1,248 K.

obtained for both samples. Large particles could be cut only from the Clear Creek shale because the Anvil Points particles severely cracked on heating. Hence, Clear Creek samples were used to obtain experimental data reflecting both intrinsic kinetics and transport effects.

Small-Particle Experiments

Intrinsic kinetics data were obtained in a Perkin-Elmer, TGS-2 thermogravimetric analysis apparatus. The original shale was first ground and sieved. Then samples consisting of about 5×10^{-6} kg (5 mg) of 48–60 mesh particles (average size = 0.27×10^{-3} m) were added to the sample holder and pyrolyzed in a helium (99.5%) atmosphere. Prior to heating the system was purged at room temperature with helium (flow rate 1.33×10^{-6} m^3/s at 273 K, 101 kPa) for three hours to eliminate oxygen. The sample weight during purging remained essentially constant and equal to the weight predetermined in a balance.

Weight vs. time data were taken at constant temperatures in the range of 673 to 718 K. Below 673 K the rate of pyrolysis is very low. High temperatures were avoided since we were interested in the kinetics of kerogen decomposition rather than that of carbonates in the shale. For Colorado shales Galan and Smith (1983) and Campbell et al. (1976a,b) found that carbonate decomposition was not appreciable below 723 K. After purging with helium, the temperature was increased from 298 K to the desired constant value by heating at the maximum rate, 2.67 K/s.

Very small samples of small particles were used in order to avoid intraparticle and interparticle temperature gradients. The sample was located at the center of the TGA furnace so that the temperature in the sample holder was uniform.

Large-Particle Experiments

Pyrolysis data for large particles were obtained in a specially constructed

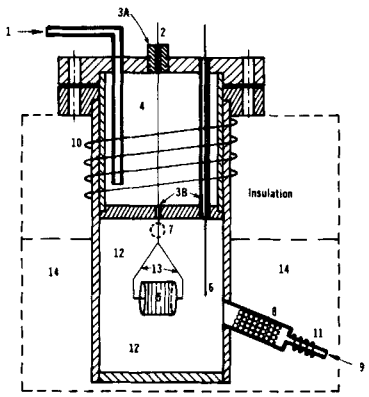

Figure 1. Reactor assembly for large particles.

TABLE 2. AXIAL GAS TEMPERATURE PROFILE IN REACTOR

Distance from bottom of reactor, m	1.5×10^{-2}	5×10^{-2}	6×10^{-2}	9.5×10^{-2}
Temperature, K	713	723.5	722	704

TGA-type apparatus, Figure 1. The reactor, furnace, and preheater assembly were similar to those employed by Galan and Smith (1983) except that modifications were made to obtain a more uniform temperature within the reactor. This was accomplished by adding a tape heater *10* (Figure 1) to the pressure chamber *4* above the reactor, adding a tape heater *11* at the preheater entrance, and using two controllable heaters in the furnace surrounding the reactor.

The reactor chamber had a diameter of 5.1×10^{-2} m and length of 11×10^{-2} m, and was constructed from a Monel tube. Nitrogen was fed into the reactor at an angle from the preheater (2×10^{-2} m ID, 5×10^{-2} m long), which was packed with 0.48×10^{-3} m stainless steel balls. The nitrogen flow rate was purged continuously through pinholes *3a,b* into the reactor to prevent pyrolysis products from escaping into the upper chamber. The total nitrogen flow into the upper chamber was 4.1×10^{-6} m^3/s, most of which passed out of the chamber through the upper pinhole.

The reactor was enclosed in the furnace up to about the level of the lower pinholes separating the upper chamber from the reactor. By adjusting the two controlled sections of the furnace and the heating tapes, it was possible to obtain a reasonably uniform temperature within the reactor. Axial variations in temperature within the furnace are shown in Table 2. It is estimated that the maximum temperature difference in the gas from the bottom to the top of the cylindrical particles was 3 K. Measurements of wall temperatures indicated a maximum temperature difference between particle surface and wall of 67°C. At our temperature level (711 K maximum gas temperature) the radiation contribution was less than 1.0% of the convective heat transfer rate to the particle.

Cylindrical samples of Clear Creek shale ($2.54 \times 10^{-}$ 2 m diam., 25.4 mm and 2.0×10^{-2} m length) were held by two prongs of stainless steel wire inserted nto the flat ends of the cylindrical particle (Figure 1). The sample holder was attached to a weighing wire (1.0×10^{-4} m dia.) leading to a Mettler H-6 digital readout balance. The shale samples were not isotropic, but consisted of reasonably well-defined layers of kerogen separated approximately by layers of rock (the usual structure for Colorado shale). The kerogen layers were perpendicular to the axis of the cylinder, as indicated by the vertical lines on the shale particle *5*, Figure 1. The particle was cut with a diamond saw from large granular pieces of shale.

During a retorting run the gas temperature was measured with an iron-constantan thermocouple whose junction was positioned at the elevation of the axis of the cylindrical particle. The insulated thermocouple wires were enclosed in a stainless steel sheath 1.59×10^{-3} m (1/16 in.) in diameter. This temperature reading was used with an Omega M-22 controller to control the temperature vs. time history.

In addition to small holes in the end faces of the shale particle, a hole was drilled to the center of the particle and a slot was drilled on the outer cylindrical surface. Thermocouples of 30-gauge iron-constantan were cemented into the central hole and the slot for measuring the center and surface temperatures of the particle. A Saureisen electrical heating cement was used. The thermocouple wires were insulated up to the junction. With this arrangement separate runs were necessary for obtaining weight vs. time and temperature vs. time data. We attempted to obtain all the data from samples which had the same kerogen content. This was accomplished by choosing samples of the same color.

Scope of Measurements

For intrinsic kinetics studies, weight and temperature vs. time were measured at four temperature levels: 673, 688, 703, and 718 K. A platinum-platinum-rhodium thermocouple was located just beneath the pan holding the shale sample.

In the large-particle experiments, gas temperatures vs. time were recorded for every run. Runs were made by heating to three plateau temperatures: 673, 693, and 711 K.

Heat transfer coefficients from gas to particle surface were measured in the same apparatus (Figure 1), but with the shale particle replaced with a solid, stainless steel cylinder of the same size. An iron-constantan, 30-gauge thermocouple was located in the center of the steel cylinder, and this temperature and that of the surrounding gas were measured vs. time. These runs were carried out in the same way as those with shale particles; that is, with nitrogen flow at room temperature the heaters were turned on and the controllers set to give the same gas-temperature vs. time history. The heat transfer coefficient was based upon the total cylindrical and end-face area (26.1×10^{-4} m^2), and was calculated from the equation

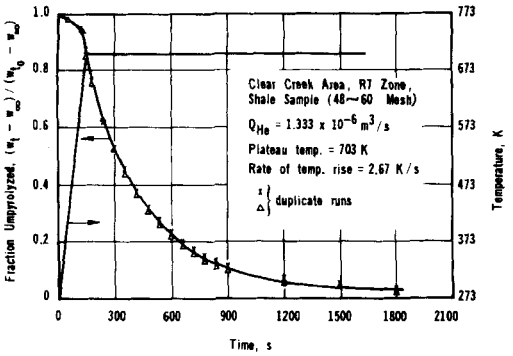

Figure 2. Reproducibility of TGA data for small particles.

$$h = \frac{(wc_p)_{\text{steel}}}{(T_g - T_{\text{steel}})A_s}\left(\frac{dT}{dt}\right)_{\text{steel}} \tag{1}$$

Measurements were made at four nitrogen flow rates in the range 4.02×10^{-6} to 35.8×10^{-6} m^3/s.

The density of the fresh and retorted shale was determined at room temperature from the mass of the particle and its volume, as obtained in a Beckman Model 930 air comparison pycnometer.

SMALL PARTICLE RESULTS—INTRINSIC KINETICS

Figure 2 illustrates the reproducibility of the weight vs. time data for the small shale particles. The runs are for two different samples from the same batch of ground particles of Clear Creek shale. The run time was continued until the weight no longer changed during the constant-temperature (plateau temperature) period; this established w_∞. The ordinate in Figure 2 is a fractional weight change based upon w_∞. This quantity $(w_t - w_\infty)/(w_{t_o} - w_\infty)$ would be equal to the fraction of the kerogen that has not been pyrolyzed (unconverted fraction) if all the products of pyrolysis were vaporized (no coke produced).

If the rate of decomposition is first-order in kerogen concentration,

$$\frac{dC_k}{dt} = -kC_k \tag{2}$$

Neglecting the change in volume during pyrolysis, the integrated form of Eq. 2 may be written

$$\ln\frac{w_t - w_\infty}{w_{t_o} - w_\infty} = -k(t - t_o) \tag{3}$$

where w_{t_o} is the weight of the sample at the start of the constant-temperature period, which is time t_o (150 s in Figure 2). Values of w_∞/w_{t_o} varied only slight with the plateau temperature. The variation was random from 0.835 to 0.856 for the Anvil Points shale

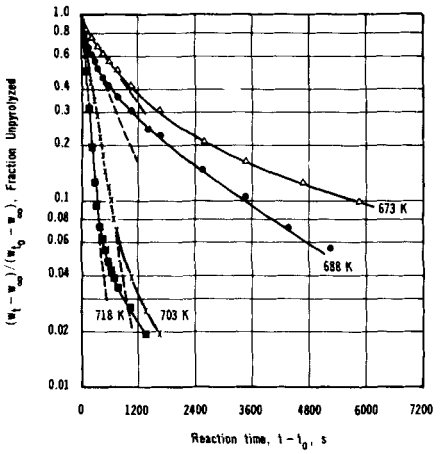

Figure 3. Fraction unpyrolyzed vs. time for Anvil Points shale (small-particle data).

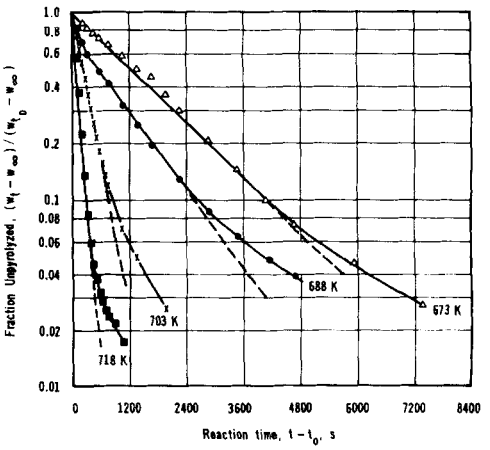

Figure 4. Fraction unpyrolyzed vs. time for Clear Creek shale (small-particle data).

and from 0.718 to 0.737 for the Clear Creek samples. Ratios w_∞/w_o, where w_o corresponds to $t = 0$, also varied but little with temperature level.

Figures 3 and 4 show the fractional weight vs. time plotted as suggested by Eq. 3. Nearly straight lines, indicating first-order kinetics, are obtained down to a fractional weight change that depends upon the temperature and is different for the two shales. Since kerogen is probably a complex mixture of complex organic molecules, deviation from first-order kinetics when most of the kerogen has been pyrolyzed is not unexpected. For example, coke-forming reactions, which would lead to larger values of the ordinate in Figures 3 and 4, could explain, in part, the concave shape of the curves at low values of $(w_t - w_\infty)/(w_{t_o} - w_\infty)$.

For evaluating k in Eq. 3, the experimental points included in the dashed straight-line sections of the curves in Figures 3 and 4 were used. Linear regression analysis gave the results indicated in Table 3. These k values are shown in an Arrhenius plot in Figure 5. The activation energies corresponding to the straight lines in Figure 5 are $E = 2.47 \times 10^5$ kJ/kg·mol for the Anvil Points shale and 2.54×10^5 kJ/kg·mol for the Clear Creek shale. It is interesting to note that despite the different origin of the shales and the different oil contents (Table 1), the rate constants and activation energies for the two shales are nearly the same.

Several other intrinsic kinetics results have been reported. For example, Johnson et al. (1975) compared first-order rate constants from their studies and those of several other investigations and also found similar results. However, their average activation energy, 1.95×10^5 kJ/kg·mol, was lower than our values. Activation energies obtained from first-order kinetics by Campbell et al. (1976a) and by Shih and Sohn (1980) were 2.14 and about 2.00×10^5 kJ/kg·mol, respectively.

The intrinsic kinetics results given in Figure 5 will be used in the prediction model for pyrolysis of the cylindrical particles.

LARGE PARTICLE RESULTS

The data for temperatures vs. time for the large cylindrical particles are illustrated in Figure 6, which is for a gas-temperature

TABLE 3. FIRST-ORDER REACTION RATE CONSTANTS

Temp. K	Rate Constant, k, s^{-1}	
	Anvil Points Shale	Clear Creek Shale
673	5.54×10^{-4}	5.12×10^{-4}
688	8.90×10^{-4}	8.70×10^{-4}
703	3.63×10^{-3}	2.84×10^{-3}
718	6.49×10^{-3}	7.29×10^{-3}
Activation Energy, kJ/kgmol	2.47×10^5	2.54×10^5

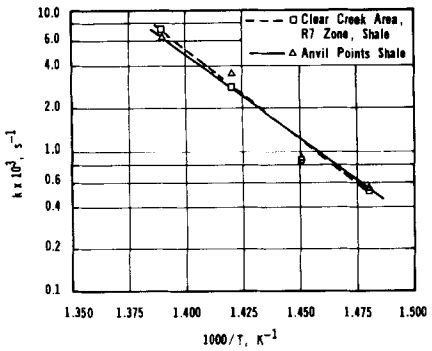

Figure 5. Arrhenius plot for small particles.

plateau of 711 K. The temperature increase of gas over particle-center temperature is zero at $t = 0$ and at long times; in between, this difference reached a maximum of about 60°C. Data for two runs at the same conditions but with different shale particles are shown in Figure 6 to indicate the reproducibility of the data.

Particle-surface temperatures were not as reproducible as the gas and particle-center values. The maximum difference between gas and particle surface was about 35°C while the maximum difference between surface and center of the particle was about 30°C, although these maximum values did not occur at the same run time. From the results it seems clear that both gas-to-particle surface and intraparticle heat transfer affect pyrolysis rates, and both transport resistances should be included in a prediction model.

Figure 7 shows the experimental data for the fractional weight change vs. time for a plateau gas temperature of 693 K. In the ordinate w_o is the sample weight at zero time. Data are shown for two runs at the same conditions but, of necessity, for different shale particles.

HEAT TRANSFER COEFFICIENTS

The data from the heat transfer experiments with the steel cylinder consisted of the temperatures of the gas and the center of the cylinder, vs. time. From these data and $(wc_p)_{steel}$ and A_s, the heat transfer coefficient could be calculated for all time intervals. The results for the first time intervals, when the temperature was low, were somewhat erratic but agreed within ± 10% at longer times when the temperature was higher (>473 K). Figure 8 is a plot of average values of h vs. nitrogen flow rate. The small effect of flow rate is perhaps due to the swirling, turbulent nature of the flow caused by the geometry of the reactor (Figure 1). The nitrogen enters at an angle through a small, packed preheater tube. The pyrolysis data were obtained for a nitrogen flow rate of 8.17×10^{-6} m^3/s (at 273 K and 101 k Pa), so that h = 33.7 $J/m^3 \cdot s \cdot K$ was used in the model predictions.

The density of fresh and of spent shale particles was measured at room temperature. The fresh shale had no measurable porosity so that the apparent density was equal to the solid phase value. This

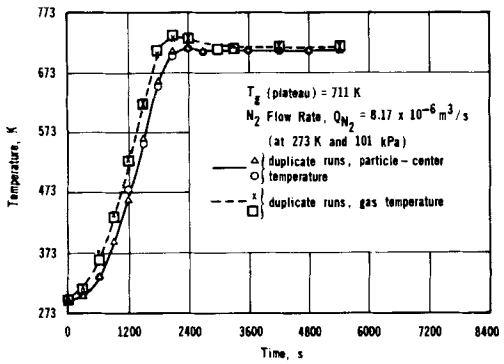

Figure 6. Experimental gas and particle-center temperatures for cylindrical particles (Clear Creek shale).

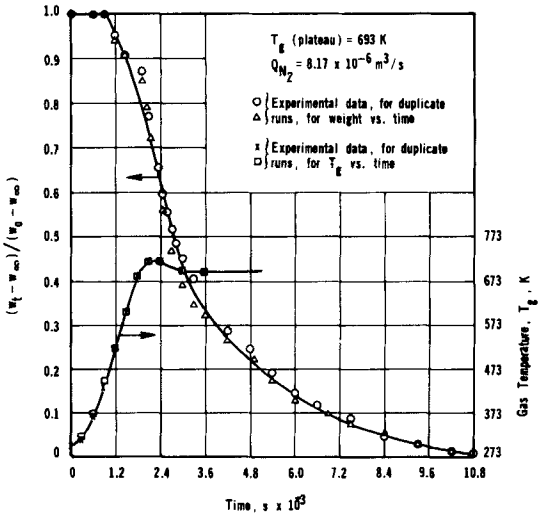

Figure 7. Weight vs. time for large particles (Clear Creek shale).

was 1,960 kg/m^3. For spent shale, solid and apparent densities were 2,740 and 1,530 kg/m^3, respectively, corresponding to a porosity of 0.440.

PYROLYSIS MODEL FOR LARGE PARTICLES

Since most of the products of pyrolysis are vapors, there is a rapid convective flow out of the layers of kerogen in the particle. This reduces intraparticle mass-transfer resistance in the direction of the kerogen layers. It is assumed that there is no mass transfer of products through the inert rock perpendicular to the layers. The significance of particle-to-gas mass transfer was predicted, approximately, by estimating the mass-transfer coefficient from particle surface to gas. These calculations suggested that the mass transfer rate was about 11 times greater than the maximum reaction rate. Accordingly, the proposed model is based only on heat transfer and intrinsic kinetics. Shih and Sohn (1978), Campbell et al. (1978), and Granoff and Nuttall (1977) have also neglected mass-transfer resistances in their models.

Additional assumptions are:

1. Gas-to-particle heat transfer can be accounted for by using the heat-transfer coefficient determined from the experiments with a steel cylinder (Figure 8).
2. The shale particle is isotropic for heat transfer, and particle volume and shape are constant.

Our model differs from that of Shih and Sohn (1980) in that they employed spherical geometry while we used a two-dimensional energy balance to account accurately for heat transfer in the cylindrical particle. Our test of the model was more critical since we measured, independently of the pyrolysis experiments, intrinsic kinetics, gas-to-particle heat transfer coefficient, and particle temperatures, and thus did not have disposable parameters with which to fit the data.

For the given restrictions the energy balance is

$$\rho_p (c_p)_p \frac{\partial T}{\partial t} = k_e \left[\frac{\partial^2 T}{\partial r^2} + \frac{1}{r} \frac{\partial T}{\partial r} + \frac{\partial^2 T}{\partial z^2} \right] - k C_k \Delta H_R \qquad (4)$$

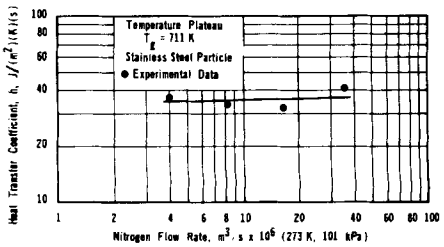

Figure 8. Heat transfer coefficient data.

TABLE 4. PARTICLE PROPERTIES USED FOR PREDICTED RESULTS

Plateau Temp. T_g K	Temperature-Rising Period $(c_p)_p$ J/kg·K	k_e J/m·K·s	ρ_p kg/m³	Constant-Temp. Period $(c_p)_p$ J/kg·K	k_e J/m·K·s	ρ_p kg/m³
673	1,010	0.942	1,960	1,060	0.545	1,750
693	1,020	0.950	1,960	1,070	0.571	1,750
711	1,030	0.958	1,960	1,080	0.599	1,750

where T is the temperature in the shale particle and $(kC_k\Delta H_R)$ is the rate of heat release per unit volume of particle. The coordinates r and z are measured from the center of the cylinder.

The initial and boundary conditions are:

$$T_g = T_o \qquad \text{at } t = 0 \tag{5}$$

$$\frac{\partial T}{\partial r} = 0 \qquad \text{at } r = 0 \tag{6}$$

$$\frac{\partial T}{\partial z} = 0 \qquad \text{at } z = 0 \tag{7}$$

$$k_e\left(\frac{\partial T}{\partial r}\right) + h(T_s - T_g) = 0 \qquad \text{at } r = r_o \tag{8}$$

$$k_e\left(\frac{\partial T}{\partial z}\right) + h(T_s - T_g) = 0 \qquad \text{at } z = L/2 \tag{9}$$

With no mass-transport resistances, the mass balance for kerogen and the initial condition are

$$\frac{dC_K}{dt} = -A\left[\exp\left(-\frac{E}{R_g T}\right)\right]C_k \tag{10}$$

$$C_k = C_{k_o} \qquad \text{at } t = 0 \tag{11}$$

The solution of these equations gives $T = f(t,r,z)$ and $C_k = f(t,r,z)$.

The fraction of the kerogen unpyrolyzed for the whole pellet can be expressed in terms of C_k as

$$f = \frac{\int_{-L/2}^{L/2}\int_0^{r_o} 2\pi r C_k (dr)(dz)}{\pi r_o^2 L C_{k_o}} \tag{12}$$

If it is again assumed that all the weight change is due to gaseous products, f is also equal to the fractional weight change.

$$f = \frac{w_t - w_\infty}{w_{30} - w_\infty} \tag{13}$$

Hence, from Eqs. 12 and 13 the fractional weight change, as observed experimentally, can also be predicted. In Eq. 13 w_{30}, the weight after 1,800 s, is taken as the sample weight when kerogen begins to decompose. This is based on the independent temperature vs. time runs where the temperature at which kerogen begins to decompose, 623 K, occurs at about 1,800 s. There is some weight loss, about 10% of the total loss, during the heating period from room temperature to 623 K. This loss is attributed to water, easily desorbed gases, and some light oil fractions. The concentration C_{k_o} needed for the solution of the equations was taken as $(w_{30} - w_\infty)/V$ where V is the known volume of the shale cylinder. Values of C_{k_o} obtained in this way were nearly the same for all plateau temperatures; the average was 330 kg of kerogen/m³ of particle.

Equations 4–11 were written in dimensionless form by introducing dimensionless variables. The solution was obtained numerically using the implicit alternating-direction, finite difference method described by Douglas and Rechford (1956). The resulting profile for C_k was then used in Eq. 12, which with Eq. 13 gave the fractional weight change for kerogen pyrolysis.

EXPERIMENTAL AND PREDICTED RESULTS

The parameters in Eqs 4–11 are A, E, C_{k_o}, h, ρ_p, $(c_p)_p$, k_e and ΔH_R. The first five were measured by us in independent experiments. The other three, $(c_p)_p$, k_e, and ΔH_R, were evaluated from literature data. The effective thermal conductivity k_e of fresh and spent shale was obtained from the correlation of Tihen et al. (1968), while the specific heat $(c_p)_p$ of fresh and spent material was obtained from Shaw (1947). Little information is available for the heat of decomposition of Colorado shale. In our predictions we used the value suggested by Shih and Sohn (1978), 3.75×10^2 kJ/kg of kerogen in the shale.

All three properties vary with temperature, but ΔH_R and ρ_p were assumed to be constant at the value given. As seen later, the predicted results are not very sensitive to ΔH_R. In the computations the h value employed was that from Figure 8 at a flow rate of 8.17 $\times 10^{-6}$m³/s. For $(c_p)_p$ and k_e, average values for fresh shale at T_o (298 K) and for spent shale at the plateau temperature were used for the temperature-rising period; for the constant-temperature

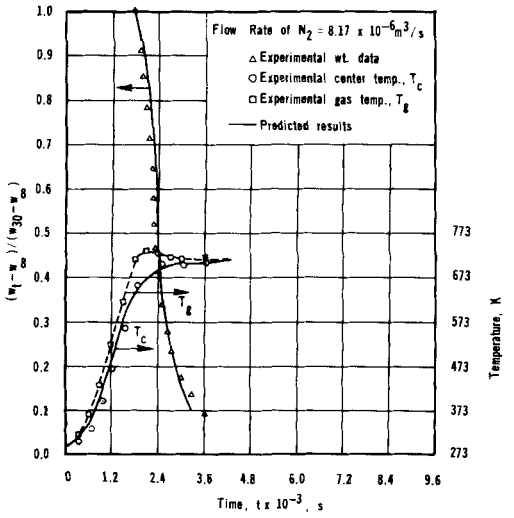

Figure 9. Predicted and experimental results for large Clear Creek shale particles for plateau temperature, T_g = 711 K.

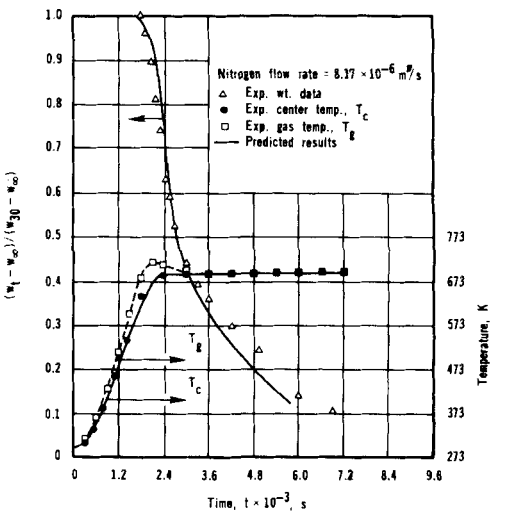

Figure 10. Predicted and experimental results for large Clear Creek shale particles for plateau temperature T_g = 693 K.

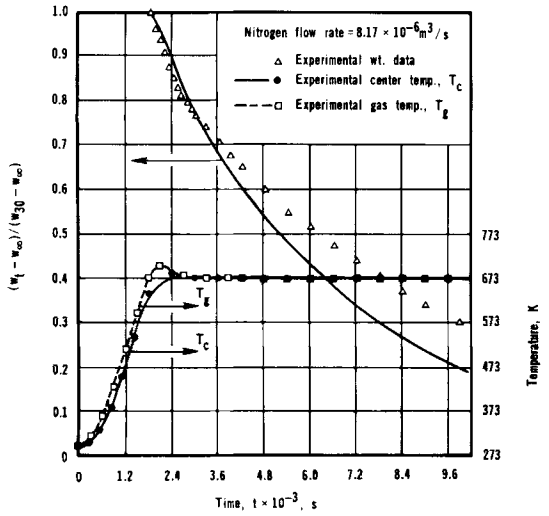

Figure 11. Predicted and experimental results for large Clear Creek shale particles for plateau temperature T_g = 673 K.

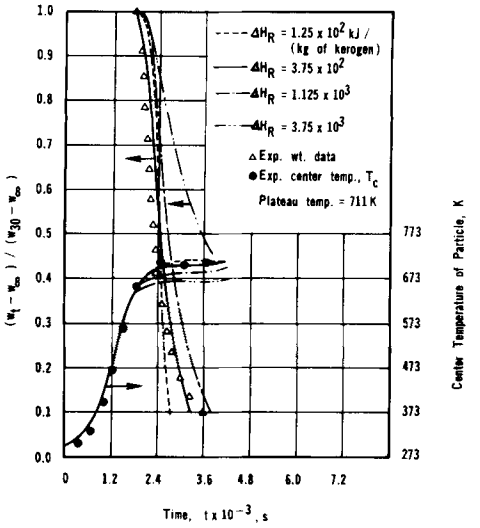

Figure 12. Sensitivity of predicted results to ΔH_R.

period, values for spent shale at the plateau temperature were used. The density ρ_p was assumed to be that of the fresh shale during the temperature-rising period and equal to the average of the spent and fresh-shale values during the constant-temperature period. The numerical values employed for $(c_p)_p$, k_e, and ρ_p are given in Table 4.

The input for the computations is C_{k_o}, T_g vs. time, and the initial temperature of the shale cylinder. This last quantity is the same as the initial gas temperature, about 295 K. The input for T_g vs. time was obtained by dividing the curve through the experimental points, such as that shown by the dashed lines in Figures 9–11, into linear sections. The characteristics of the reactor system and nitrogen flow determined the heating rate.

Figures 9–11 show predicted and experimental fractional-weight changes $(w_t - w_\infty)/(w_{30} - w_\infty)$ and particle-center temperatures for the three plateau (T_g) temperatures. In all three figures the predicted and experimental temperatures at the center of the particle are in good agreement, considering the sensitivity of temperatures and the several independent sets of experimental data involved in the calculations. Also, the agreement is satisfactory for the fractional weight change over the whole range from 1.0 to 0.1 for a plateau temperature of 711 K (Figure 9). However, predicted and experimental weight-change fractions deviate at the lower levels for plateau temperatures of 693 and 673 K (Figures 10 and 11). Furthermore, the deviation increases as the fraction of unconverted kerogen decreases, that is, as $(w_t - w_\infty)/(w_{30} - w_\infty)$ decreases, and the extent of deviation is greatest for the lowest plateau temperature (Figure 11). These same trends are observed in the intrinsic kinetics results shown in Figure 4 for the Clear Creek shale. Deviations from first-order pyrolysis become more pronounced as the fraction unconverted decreases, and the deviation begins at higher fractions unconverted the lower the temperature. Therefore, using the experimental intrinsic kinetics data in Figure 4, rather than the first-order correlation, would have decreased the deviation between experimental and predicted values of $(w_t - w_\infty)/(w_{30} - w_\infty)$. However, Figure 4 shows that it is only at values of the fraction unconverted less than 0.1 that deviations from first-order behavior occurred. Hence, this leaves unexplained the deviations in Figures 10 and 11 at $(w_t - w_\infty)/(w_{30} - w_\infty)$ greater than 0.1. Possible reasons include the longer reaction times required to reduce the fractional weight change at the lower temperatures, because this may result in more carbon deposited. Coke formation is known to increase with time in thermal cracking of petroleum fractions. If this occurred, the fractional weight change would be less than predicted since our model does not account for deposited carbon product. Note that the time required to reach a fraction unconverted of 0.3 is nearly 10,000 s at a plateau temperature of 673 K but only about 2,800 s at 711 K (Figure 9). Also, the model is rather approximate. For example, it is assumed that the shale is isotropic for heat transfer. While k_e is probably not the same in all directions in the particle it seems unlikely that the deviations, which occur only at low fractions unconverted, are due to this assumption.

As noted earlier, values of $(c_p)_p$, k_e, and ΔH_R were not measured in our work but taken from the literature. Hence, it is useful to know the effect of these properties on the predicted results. Figure 12 shows the sensitivity of the particle-center temperature and the weight-fraction unconverted to the heat of reaction. Results for ΔH_R ranging from one-third to ten times the chosen value of 3.75 $\times 10^2$kJ/kg of kerogen are shown. Also shown are the experimental data. It is seen that a very large change in ΔH_R would not affect the results more than the expected uncertainty in the experimental data. Describing the matter differently, the experimental procedure is not a suitable method for evaluating the heat of reaction. Similar computations show that the results during the temperature-rising period are most sensitive to $(c_p)_p$. A 50% change in $(c_p)_p$ introduces a greater difference in $(w_t - w_\infty)/(w_{30} - w_\infty)$ than a threefold change in ΔH_R. The results during the temperature-rising period are least sensitive to k_e because the temperature gradient within the particle is not large. On the other hand, the sensitivity of the fraction unconverted to the heat transfer coefficient h is only slightly less than the sensitivity to $(c_p)_p$.

ACKNOWLEDGMENT

We thank the government of China for fellowship support. Also, the financial support of National Science Foundation Grant 80-26101 is gratefully acknowledged. The preliminary studies of M.A. Galan were beneficial.

NOTATION

a = frequency factor, s^{-1}
A_s = total outer surface area of steel particle, m^2
C_k = concentration of kerogen in shale particle, kg/m^3 of total particle
C_{k_o} = concentration at time when decomposition of kerogen begins
$(c_p)_p$ = specific heat of shale particle, J/kg·K
$(c_p)_{steel}$ = specific heat of stainless steel, J/kg·K

E = activation energy for kerogen decomposition, J/gmol
f = fraction of kerogen pyrolyzed
h = average heat transfer coefficient between gas and particle, J/m^2·K·s
ΔH_R = heat of pyrolysis of kerogen, kJ/kg of kerogen
k = first-order reaction rate constant, s^{-1}
k_e = thermal conductivity of particle of shale, J/m·K·s
L = length of cylindrical particle of shale, m
Q = volumetric gas flow rate, m^3/s at 273 K and 101 kPa
R_g = gas constant, J/gmol·K
r = radial distance measured from axis of cylindrical particle, m
r_o = radius of particle
T = temperature within shale particle, K
T_c = temperature at center of particle
T_g = gas temperature, K
T_o = temperature of gas or particle at $t = 0$
T_s = temperature at outer surface of shale particle
T_{steel} = temperature of steel particle, K
t = time, s
t_o = time at beginning of constant-temperature period
V = volume of shale particle (cylinders), m^3
w_t = total weight of shale sample or particle at time t, kg
w_∞ = total weight when weight no longer changes with time, kg
w_o = total weight at $t = 0$
w_{t_o} = total weight of sample at beginning of constant-temperature period in experiments with small particles, kg
w_{30} = total weight of particle at $t = 1{,}800$ s, kg
w_{steel} = weight of steel particle, kg
z = axial distance in large shale particle, measured from center, m

Greek Letters

ρ_p = density of shale particle, kg/m^3

LITERATURE CITED

Allred, V. K., "Kinetics of Oil Shale Pyrolysis," *Chem. Eng. Prog.*, **62**, 55 (1966).

Campbell, J. H., G. Koskinas, and N. Stout, "The Kinetics of Decomposition of Colorado Oil Shale. I: Oil Generation," Lawrence Livermore Laboratory UCRL-52089 (1976a).

Campbell, J. H., "The Kinetics of Decomposition of Colorado Oil Shale. II: Carbonate Mineral," Lawrence Livermore Laboratory UCRL-52089, Part 2 (1976b).

Campbell, J. H., G. H. Koskinas, and N. D. Stout, "Oil Shale Retorting: Effects of Particle Size and Heating Rate on Oil Evolution and Intraparticle Oil Degradation," *In Situ*, **2**(1), 1 (1978).

Douglas, J., and H. H. Rechford, "On the Numerical Solution of Heat Conduction Problems in Two- and Three-Space Variables," *Trans. Amer. Math. Soc.*, **82**, 421 (1956).

Finuchane, D., J. H. George, and H. G. Harris, "Pertubation Analysis of Second-Order Effects in Kinetics of Oil Shale Pyrolysis," *Fuel*, **56**, 65 (1977).

Galan, M. A., and J. M. Smith, "Pyrolysis of Oil Shale—Experimental Study of Transport Effects," *AIChE J.*, **29**, 604 (1983).

Granoff, B., and H. E. Nuttall, "Pyrolysis Kinetics for Oil-Shale Particles," *Fuel*, **56**, 234 (July, 1977).

Hubbard, A. B., and W. E. Robinson, "Thermal Decomposition Study of Colorado Oil Shale," *Rept. of Invest. 4744*, U.S. Bur. Mines (Nov. 1950).

Johnson, W. F., et al., "In Situ Retorting of Oil Shale Rubble: A Model of Heat Transfer and Product Formation in Oil Shale Particles," *Q. Colorado Sch. Mines*, **70**, (3), 237 (1975).

Nuttall, H. E., et al., "Pyrolysis Kinetics of Several Key World Oil Shales," *Geochemistry and Chemistry of Oil Shales*, AGS Symp. Ser. **230**, (1983).

Shih, S. M., and H. W. Sohn, "Non-Isothermal Determination of the Intrinsic Kinetics of Oil Generation from Oil-Shale," *I&E.C., Proc. Des. Dev.*, **19**, 420 (1980).

Tihen, S. S., H. C. Carpenter, and H. W. Sohn, "Thermal Conductivity and Thermal Diffusivity of Green River Oil Shale," Proc. 7th Conf. Thermal Conductivity, *SP Pub. 302*, 529 Nat. Bur. Stds., (1968).

Shaw, R. J., "Specific Heat of Colorado Oil Shales," *Rept. of Invest. 4151*, U.S. Bur. Mines (1947).

Wise, R. L., R. C. Miller, and H. W. Sohn, "Heat Contents of Some Green River Oil Shales," *Rept. of Invest. 7482*, U.S. Bur. Mines (1971).

Manuscript received Aug. 9, 1983; revision received Apr. 23, 1984, and accepted Apr. 30.